Mass Transfer Mechanism of Ion Exchange in Fixed Bed Columns

Indianara C. Ostroski,[*][†] Carlos E. Borba,[‡] Edson A. Silva,[§] Pedro A. Arroyo,[†] Reginaldo Guirardello,[‡] and Maria A. S. D. Barros[†]

[†]Chemical Engineering Department, State University of Maringá, 5790 Colombo Av., Bl. D-90, 87020-900 Maringá, PR, Brazil

[‡]School of Chemical Engineering, State University of Campinas, UNICAMP, University City Zefenino Vaz, P.O. Box 6066, 13081-970 Campinas, SP, Brazil

[§]Chemical Engineering Department, West Paraná State University, 645 Faculdade Street 645, Jardim La Salle, 85903-000 Toledo, PR, Brazil

ABSTRACT: In this work, the binary ion exchange of $Zn^{2+}-Na^+$ ions has been studied by a column technique using a NaY zeolite as the cation exchanger. The experimental data (breakthrough curves) for the binary system were obtained at total concentrations of (1, 2, and 3) $meq \cdot L^{-1}$. The mass action law was used to represent the ion exchange equilibrium. To represent the ion exchange in the column, two models were used. In the first model, the rate-controlling step of mass transfer was considered only in the solid phase. The experimental results were represented by a Linear Driving Force (LDF) model. In the second model, resistance to mass transfer in series in the solid phase and the external liquid film was considered. Both models described ion exchange in the fixed-bed column properly. However, in the initial part of the breakthrough curve, the dual resistance model fit better.

INTRODUCTION

Zinc is the third nonferrous metal most consumed after copper and aluminum. Its use is wide due to its properties that include high resistance to corrosion and excellent quality and versatility of its alloys.

Wastewater containing zinc may be treated through different processes. Recovery of Zn(II) can be done by a precipitation process,[1] but some zinc concentrations are still detectable in the fluid phase after this operation. Therefore, a complementary treatment is needed. Ion exchange is one of such treatments. However, Na is also present in most wastewaters and may influence the removal of zinc due to changes in the diffusion process toward the ion exchange sites.

Zeolites are proven ion-exchanging materials, where the indigenous (typically sodium) charge balancing cations can be easily exchanged with cations in solution.[2] Zeolites have been already successfully applied in the single removal of heavy metals such as Cr^{3+}, Fe^{3+}, Co^{2+}, and Zn^{2+}.[3-6]

Ion-exchange equilibrium in zeolites is a function of the solid- and aqueous-phase composition. As these parameters can vary substantially for the chemical system of interest, it is essential to have models that allow accurate description of the experimental data.[7] One of the most accurate models is the mass action law. It treats ion exchange as a reversible reaction where the valences of the counterions are the stoichiometric coefficients.[8] Like any chemical reaction, the equilibrium constant can be written based on the stoichiometry and provides a measure of the relative selectivity of a sorbent for two exchanging ions.[9] In the mass action law model, the activity coefficients for the electrolytes in the solution phase and in the solid phase must be known. These coefficients can be estimated using the Bromley[10] and Wilson[11] methods.

Besides equilibrium behavior, phenomenological models in packed beds should be also applied to estimate the dynamic behavior of ion exchange. Previous work has already investigated

Table 1. Characterization of the Zeolite NaY

zeolite	% SiO$_2$	% Al$_2$O$_3$	% Na$_2$O	Si/Al	% dry mass
NaY	66.4	19.9	12.6	2.83	81.9

zinc removal in a NaY column using adsorption models.[6] Now, this work aims to improve the understanding of zinc removal in a zeolite NaY packed bed. Therefore, the mass action law was used to estimate the equilibrium data and was applied for the dynamic ion exchange by considering two models. In the first model the rate-controlling step of mass transfer was considered only in the solid phase, and this was represented by a Linear Driving Force (LDF) model. In the second model, resistance to mass transfer in series in the solid phase and the external liquid film formed around the exchanging ion particles was considered.

EXPERIMENTAL SECTION

Zeolite. All experiments were carried out with a NaY powder without binder, which has the unit cell composition Na$_{81}$-(AlO$_2$)$_{81}$(SiO$_2$)$_{111}$ (122 % crystalline) based on XRD and XRF results. The cation exchange capacity (CEC) was calculated to be 3.9 $meq \cdot g^{-1}$ according to the aluminum content.[12] To ensure the complete exchange of any different balancing cation for sodium ions, the parent zeolite, as received, was contacted with 1 $mol \cdot L^{-1}$ NaCl at 60 °C and a zeolite-solution ratio of 1:10. Then, the sample was washed with hot deionized water and oven-dried at 100 °C. This procedure was repeated four times.[13] The percentage of dry mass was obtained by calcination of the sample at 815 °C. Table 1 shows the results of the zeolite

ACS Publications © 2011 American Chemical Society

375

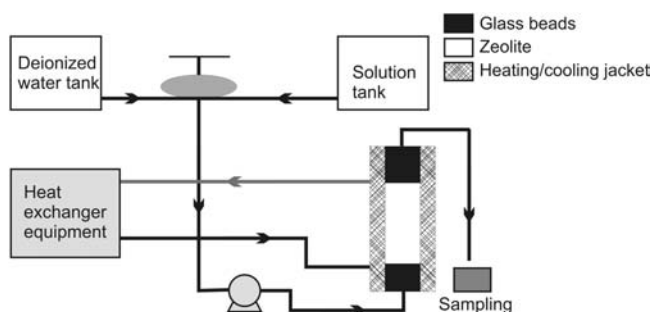dx.doi.org/10.1021/je100568n | J. Chem. Eng. Data 2011, 56, 375–382

Figure 1. Flow diagram for dynamic ion-exchange studies.

characterization. The NaY samples were pelletized, screened, and collected in an average diameter size of 0.18 mm as previously recommended as the optimal particle size for this fixed-bed system.[12]

Reagent and Solution. Reagent-grade $ZnCl_2$ and NaCl were mixed with deionized water to prepare the synthetic solutions for the dynamic runs. The experimental breakthrough data were obtained at different total feed concentrations of (1, 2, and 3) $meq \cdot L^{-1}$ ($Zn^{2+}-Na^+$) and in the following equivalent fractions of zinc: 0.10, 0.30, 0.50, 0.70, and 0.90. All pH values for the feed solutions were corrected to 4.5 using 1 M NaOH or 1 M HCl solutions when necessary. The sodium and zinc concentrations in the fluid phase were determined by atomic absorption spectrophotometry using a Varian spectrophotometer. The standards employed were prepared from stock solutions.

Ion-Exchange Unit. The ion-exchange unit where the dynamic experiments were performed is shown in Figure 1. The ion-exchange column consisted of a clear glass tube with 0.9 cm ID and 30 cm long, with the zeolite pellets supported by glass beads. The column was connected to heat exchange equipment that maintained the system at 30 °C. Before starting the runs, the zeolite bed was rinsed by pumping deionized water up flow through the column. The procedure was stopped when air bubbles could no longer be seen. After the bed placement at a bed height of 3.0 cm, which is equivalent to 0.8 g of zeolite pellets, the column was completed with glass beads. At this time, the ion exchange had started by pumping the solution up flow. Samples at the column outlet were collected regularly up to the bed saturation, and their zinc concentration was analyzed. The sodium content in the outlet samples was obtained through a mass balance in the column. The operating conditions and properties of the bed used in obtaining the breakthrough curves are shown in Table 2.

All breakthrough curves were plotted taking into account the cation concentration in the outlet samples as a function of the running time.

The amount of zinc retained along the column by the zeolite NaY was calculated from the following equation[14]

$$q_{Zn}^* = \frac{C_{Zn}^0 \dot{Q}}{1000 \cdot m} \int_0^t (1 - C_{Zn}|_{z=L}/C_{Zn}^0) dt \qquad (1)$$

where q_{Zn}^* is the equilibrium concentration of Zn(II) ($meq \cdot g^{-1}$); Q is the volumetric flow rate of the solution ($mL \cdot min^{-1}$); $C_{Zn}|_{z=L}$ is the Zn(II) ion concentration at the column outlet ($meq \cdot L^{-1}$); C_{Zn}^0 is the feed concentration of Zn(II) ions at the column inlet ($meq \cdot L^{-1}$); m is the dry mass of zeolite (g); L is length of the bed (cm); t is time (min); and z (cm) is the length coordinate.

Table 2. Operating Conditions and Bed Properties (pH = 4.5 and T = 30 °C)

Q ($mL \cdot min^{-1}$)	C ($meq \cdot L^{-1}$)	x_{Zn}	ρ_L	ε
8.00	3.00	0.13 0.52 0.76 0.93	419.40	0.25

■ MATHEMATICAL MODELING

Modeling Ion Exchange Equilibria. The ion exchange reaction is a stoichiometric process, in that an ion in the solid phase is replaced for an equivalent ion from the solution. Therefore, the reversible reaction for the binary system $Zn^{2+}-Na^+$ can be represented by the following equation

$$Zn_S^{2+} + 2Na_R^+ \leftrightarrow Zn_R^{+2} + 2Na_S^+ \qquad (2)$$
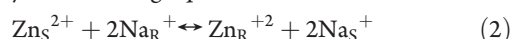
where the indexes R and S indicate the solid and the solution phases, respectively.

The thermodynamic equilibrium constant (K_{Zn}^{Na}) for the ion exchange reaction between the species Zn^{2+} and Na^+ is defined by eq 3

$$K_{Zn}^{Na} = \left(\frac{a_{R_{Zn}}}{a_{S_{Zn}}}\right)\left(\frac{a_{S_{Na}}}{a_{R_{Na}}}\right)^2 \qquad (3)$$

where a_{R_j} and a_{S_j} are the activities of ionic species in the zeolite and solution phases, respectively.

The thermodynamic equilibrium constant, defined in eq 3, can be expressed in terms of the ion activity involved in the exchange. Then, eq 3 becomes

$$K_{Zn}^{Na} = \left(\frac{y_{Zn}\gamma_{R_{Zn}}}{C_{Zn}\gamma_{S_{Zn}}}\right)\left(\frac{C_{Na}\gamma_{S_{Na}}}{y_{Na}\gamma_{R_{Na}}}\right)^2 \qquad (4)$$

where y_j is the ionic fraction of species j in the zeolite phase; C_j is the equivalent concentration of species j in the solution phase; and γ_{S_j} and γ_{R_j} are the activity coefficients of j in the zeolite and solution phases, respectively.

When considering the nonideal behavior in both phases it is necessary to estimate the activity coefficients of both species in solution and solid phases.

Activity Coefficient in the Solution Phase. The model proposed by Bromley[10] is efficient in calculating the activity coefficient of strong electrolytes in solutions with ionic strength up to 6 $mol \cdot kg^{-1}$.[15,16]

The Bromley method considers the effect of all species (cations + anions) in the solution. The expression for calculating the activity coefficient is[10]

$$\ln \gamma_{S_j} = \frac{-A z_j^2 \sqrt{I}}{1 + \sqrt{I}} + F_j \qquad (5)$$

where A is the Debye–Hückel constant. This parameter depends on temperature and is given by Zematis et al.[16] The parameter I represents the ionic force for aqueous solutions, and it can be calculated using the following equation

$$I = \frac{1}{2}\sum_{j=1}^{n} z_j^2 M_j \qquad (6)$$

where n is the number of ionic species in solution and M_j is the molal concentration of species j in the solution.

The term F_j is the interaction parameter sum and can be obtained by the following equation:

$$F_j = \sum_i B_{ji}^{\bullet} Z_{ji}^{2} C_i \tag{7}$$

where

$$Z_{ji} = \frac{z_i + z_j}{2} \tag{8}$$

$$B_{ji}^{\bullet} = \frac{(0.06 + 0.6B_{ji})|z_i z_j|}{\left(1 + \frac{1.5}{|z_i z_j|}I\right)^2} + B_{ji} \tag{9}$$

B_{ji} is the Bromley parameter of the electrolyte formed from the cation j and anion i. These values are presented elsewhere.[10]

Activity Coefficient in the Exchange Phase. Several researchers[17−25] have successfully used the Wilson[11] model to calculate the activity coefficients of ionic species in the solid phase.

The Wilson model for the estimation of the activity coefficient of species i in the solid phase is given by[11]

$$\ln \gamma_{R_i} = 1 - \ln\left(\sum_{j=1}^{h} y_j \Lambda_{ij}\right) - \sum_{k=1}^{h} \left[\frac{y_k \Lambda_{ki}}{\sum_{j=1}^{h} y_i \Lambda_{kj}}\right] \tag{10}$$

where y_i is the fraction of ionic species i in the solid phase; h is the number of species present in the solid phase; and Λ is the interaction parameter of the Wilson model. The parameters of the Wilson model are set so that $\Lambda_{ij} = 1$ when $i = j$ and $\Lambda_{ij} > 0$ when $i \neq j$. If the solid phase displays ideal behavior, we assign $\Lambda_{ij} = 1 = \Lambda_{ji}$ for any i and j.[18] For a binary system, only two parameters are needed to calculate the activity coefficients in the solid phase.

Parameter Identification Method. Besides the activity coefficients provided by the Wilson model, the thermodynamic equilibrium constant is required to estimate the ion exchange isotherm of the $Zn^{2+}-Na^+$ system from the mass action law.

This parameter can be estimated by a nonlinear identification procedure and the experimental data obtained from mass balance in the packed bed. The values of the parameters (K_{ZnNa}, Λ_{ZnNa}, Λ_{NaZn}) were obtained during the search of a minimum for the following objective function

$$F_{OBJ} = \sum_{i=1}^{h} \left[\sum_{j=1}^{M} (y_{ji}^{exp} - y_{ji}^{mod})^2\right] \tag{11}$$

where M is the number of the equilibrium data sets and h is the number of ionic species in zeolite. In the search procedure, the optimization method of Nelder and Mead,[26] coded in Fortran, was used.

Dynamic Modeling of Ion Exchange in a Fixed-Bed Column. Mathematical modeling has a key role in the scale up of any procedure from laboratory experiments through a pilot plant to industrial scale. Adequate models can help to analyze and explain experimental data, to identify the relevant mechanisms of the process, to predict changes due to different operating conditions, and to optimize the overall process productivity.[14]

In the mathematical model development of the ion exchange between Zn^{2+} and Na^+ ions in the fixed bed column, some assumptions were made:

- The hydrodynamics of the fixed bed column was described using the diffusion model in a nonstationary state.
- Two types of resistance to mass transfer in the process of ion exchange were considered. At first, it was considered that the ion exchange process is intraparticle diffusion controlled. Then, intraparticle and film resistances were considered.
- The LDF model was used to describe the concentration profiles of particles.
- The mass action law was used to represent the equilibrium in the solid/liquid interface.
- The process occurs in isothermal and isobaric conditions.
- Physical properties of the ion exchanger and the liquid phase are constant.
- Radial dispersion in the fixed-bed column is negligible.

These considerations were accomplished to mass balance ions in the liquid and solid phases to obtain the model. The equations that describe the mathematical model of the ion exchange column in the bed are given below.

The mass balance for the components Zn^{2+} and Na^+, in an element of volume in the fixed-bed column, is represented by the following equation

$$\frac{\partial C_i}{\partial t} + u_0 \frac{\partial C_i}{\partial z} + \rho_L \frac{1}{\varepsilon} \frac{\partial q_i}{\partial t} - D_L \frac{\partial^2 C_i}{\partial z^2} = 0 \tag{12}$$

in which C_i is the concentration of species i in the liquid phase $(meq \cdot L^{-1})$; q_i is the concentration of species i in the zeolite; ρ_L is the bed density $(g \cdot L^{-1})$; u_o is the interstitial velocity of the liquid phase $(cm \cdot min^{-1})$; D_L is the axial dispersion mass transfer coefficient $(cm^2 \cdot min^{-1})$; ε is the total voidage; t is the time (min); and z (cm) is the space coordinate.

Equations 13 and 14 representing the mass transfer of the external liquid film for the Zn^{2+} and Na^+ ions are, respectively

$$\frac{\partial q_{Zn}}{\partial t} = \frac{K_{FZn} \varepsilon}{\rho_L} (C_{Zn} - C_{Zn}^*) \tag{13}$$

$$\frac{\partial q_{Na}}{\partial t} = -\frac{\partial q_{Zn}}{\partial t} \tag{14}$$

where K_{Fj} is liquid film external mass transfer coefficient (min^{-1}) and C_{Zn}^* is the concentration of species Zn^{2+} in the liquid phase at equilibrium $(meq \cdot L^{-1})$.

Equations 15 and 16 represent the mass transfer inside the particle of the ion exchanger

$$\frac{\partial q_{Zn}}{\partial t} = K_{SZn}(q_{Zn}^* - q_{Zn}) \tag{15}$$

$$\frac{\partial q_{Na}}{\partial t} = -\frac{\partial q_{Zn}}{\partial t} \tag{16}$$

where K_{Sj} is mass transfer coefficient in zeolite (min^{-1}) and q_{Zn}^* is the concentration of species Zn^{2+} in the zeolite at equilibrium $(meq \cdot g^{-1})$.

The initial average concentration of ions Zn^{2+} and Na^+ in the liquid phase are presented, respectively, in

$$C_{Zn}(z,0) = 0 \tag{17}$$

$$C_{Na}(z,0) = 0 \tag{18}$$

377

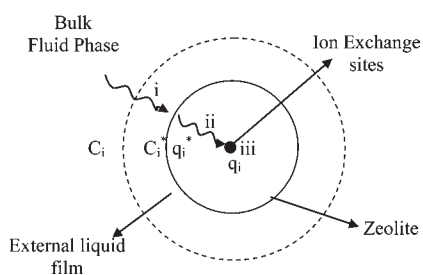dx.doi.org/10.1021/je100568n |*J. Chem. Eng. Data* 2011, 56, 375–382

Figure 2. Ion exchange process steps.

The initial concentration of ions Zn^{2+} and Na^+ in the solid phase are presented, respectively, in

$$q_{Zn}(z,0) = 0 \tag{19}$$

$$q_{Na}(z,0) = CEC \tag{20}$$

where CEC is the cation exchange capacity of the ion in the NaY zeolite.

The boundary conditions used for ion concentration of Zn^{2+} and Na^+ were as follows[27]

$$D_L \frac{\partial C_i}{\partial z} = u_0(C_i(t,0) - C_{i0}) \qquad z = 0 \tag{21}$$

$$\frac{\partial C_i}{\partial z} = 0 \qquad z = L \tag{22}$$

where C_{i0} is the feed concentration of species i in the liquid phase $(meq \cdot L^{-1})$.

Equations 12, 21, and 22 are valid for both ionic species.

The relationship between q_i^* and C_i^* is represented by the mass action law. The mathematical expression of the mass action law for the $Zn^{2+}-Na^+$ system is given by eq 4.

In the mathematical modeling of the ion exchange process in the fixed-bed column, it was assumed that the particles of the exchanger ions are spherical in shape and consist of micropores only. Thus, the mass transfer mechanism in the process of ion exchange is: (i) diffusion of ions from the bulk phase through the liquid film; (ii) diffusion of ions into the micropores of the ion exchanger; (iii) ion exchange reaction. These steps are illustrated in Figure 2.

In this work, the intraparticle resistance model and the film and intraparticle model are considered representatives of the ion exchange process. In the first model, intraparticle resistance is the rate-controlling step, and $C_i \cong C_i^*$. It applies to eqs 4, 12, and 15 to 22. In the second model, the film and intraparticle resistances are the controlling steps, and eqs 4 and 12 to 22 are used. In both cases, the rate of the exchange reaction was assumed to be rapid, and its resistance was neglected.

The mathematical models were solved using the finite volume technique. The differential partial equations were discretized with respect to the spatial coordinate z, resulting in an ordinary differential equation set with relation to time. The system of ordinary differential equations, together with their control and initial conditions, was solved using the subroutine DASSL developed by Petzold[28] and coded in Fortran.

In the mathematical models tested, three groups of parameters can be distinguished. Those that are determined experimentally $(\rho_L, \varepsilon, u_0)$ belong to the first group. The second group includes the parameters (K_{Fi}, D_L) calculated from empirical correlations.

Table 3. Thermodynamic Equilibrium Constant, Wilson Binary Interaction Parameters, and Objective Function (F_{OBJ})

system	K_{Zn}^{Na}	Λ_{Zn-Na}	Λ_{Na-Zn}	F_{OBJ}
$Zn^{2+}-Na^+$	1.6550	7.2344	0.1416	0.0294

The third group includes the parameters Λ_{Zn-Na}, Λ_{Zn-Na}, K_{Zn}^{Na}, and K_{Si} obtained through a nonlinear procedure to identify the experimental data a using statistical method of least-squares. K_{Si} was obtained using the breakthrough experimental data, while the parameters Λ_{Zn-Na}, Λ_{Zn-Na}, and K_{Zn}^{Na} were obtained using experimental equilibrium data.

The axial dispersion coefficient was estimated using the following correlation[29]

$$\frac{D_L}{u_0 d_p} = \frac{20}{\varepsilon}\left(\frac{D_m}{u_0 d_p}\right) + \frac{1}{2} \tag{23}$$

where D_m is the molecular diffusion of species in water and d_p is the zeolite average particle diameter.

The overall mass transfer coefficient in the liquid outside the film (K_{Fi}) was calculated from the correlation proposed by Wilson and Geankoplis[30]

$$J_D = \frac{1.09}{\varepsilon}(Re)^{-2/3} \tag{24}$$

where

$$J_D = \frac{k_{f_i}}{u_0}(Sc)^{2/3} \tag{25}$$

$$K_{Fi} = a_e k_{f_i} \tag{26}$$

$$a_e = \frac{6(1-\varepsilon_p)}{d_p} \tag{27}$$

J_D stands for the Chilton−Colburn factor. Re and Sc are the Reynolds number and the Schmidt number, respectively. k_{f_i} is the mass transfer coefficient in liquid film; K_{Fi} is the volumetric mass transfer coefficient in the liquid film; and a_e is the particle specific area.

Parameter Identification Method. The parameter model was estimated by the nonlinear identification procedure using the experimental data and least-squares statistical method to form the objective function (criterion). The parameter model value (K_{Si}) was obtained during the search of minima of the following objective function

$$F_{OBJ} = \sum_{j=1}^{n_d} \sum_{i=1}^{n_c} (C_{ij}^{exp} - C_{ij}^{mod})^2 \tag{28}$$

where n_d is the number of experimental data of the breakthrough curves; n_c is the number of components; C_{ij}^{exp} is the concentration of component i in the outlet of the column experimentally obtained; and C_{ij}^{mod} is the concentration of component i in the outlet of the column calculated by the mathematical model.

In the search procedure, the optimization method of Nelder and Mead[26] coded in Fortran was used.

Mathematical models with different rate-controlling steps were adjusted to breakthrough curves of the total feed concentration of 3 $meq \cdot L^{-1}$.

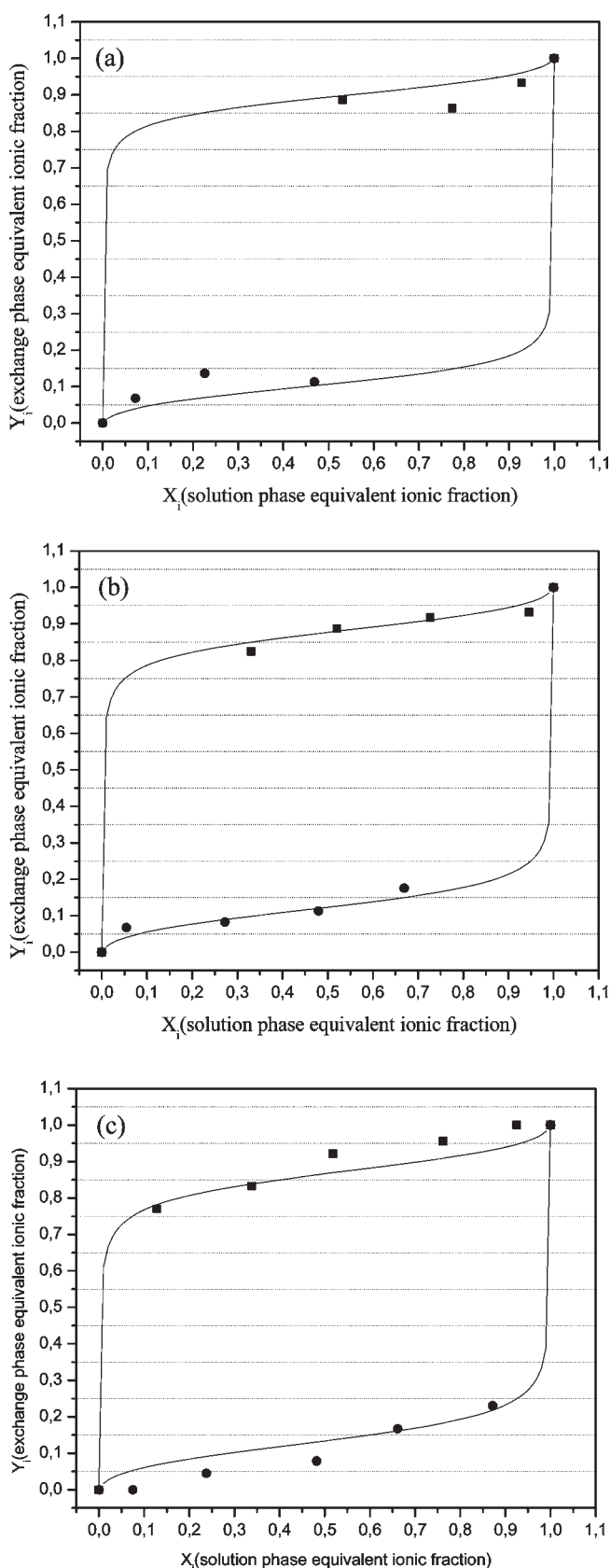**Figure 3.** Isotherm for the system Zn^{2+}/Na^+, T = 30 °C. ●, Experimental Zn^{2+}; ■, experimental Na^+; —, model (Mass Action Law): (a) C_t = 1 meq·L^{-1}; (b) C_t = 2 meq·L^{-1}; (c) C_t = 3 meq·L^{-1}.

Table 4. Experimental and Calculated Zn^{2+} Uptake Capacity

	q_{Zn}^* (meq·g^{-1})	q_{Zn}^* (meq·g^{-1})	
x_{Zn}	experimental data	model	deviation (%)
0.13	2.23	2.28	2.02
0.52	2.67	2.52	4.36
0.76	2.77	2.71	2.11
0.93	2.90	2.83	2.37

Table 5. Evaluated Parameter Values of the Model

	K_{Si} (min^{-1})	K_{Si} (min^{-1})
x_{Zn}	intraparticle resistance	film and intraparticle resistance
0.13	0.008	0.009
0.52	0.025	0.028
0.76	0.070	0.075
0.93	0.090	0.100

■ RESULTS AND DISCUSSION

Ion Exchange Equilibria. The numerical values of parameters used in the Bromley model were A = 0.5162, B_{ZnCl2} = 0.0364, and B_{NaCl} = 0.0574 at 25 °C. The parameter values are tabulated and presented by Bromley.[10]

The Wilson model, described in the section Activity Coefficient in the Exchange Phase, was used to calculate the activity coefficients of cations in the solid phase. Table 3 shows the calculated values.

In Figures 3a to 3c results of the ion exchange equilibrium obtained experimentally and simulated by the mass action law are shown. It is possible to observe that the zeolite prefers Zn^{2+} instead of Na^+, as already expected as divalent ions are preferably attracted to the negative zeolitic sites.[2]

The medium absolute error (eq 29) has been used to evaluate the equilibrium data efficiency.

$$ADD = \frac{1}{n_d} \sum_{j=1}^{n_d} \left(\frac{y_j^{exp} - y_j^{mod}}{y_j^{exp}} \right) \cdot 100 \qquad (29)$$

where y_j^{exp} is the ionic fraction of species j obtained experimentally and y_j^{mod} is the ionic fraction of species j calculated by the model.

The absolute average errors calculated were 3.82 % for Zn^{2+} and 20.3 % for Na^+. In spite of such large deviations, these values show that the mass action law represented adequately the experimental equilibrium data. Such a result was expected since the main mechanism of cation retention in zeolitic sites seems to be the ion exchange process, which is successfully described by the stoichiometric reaction and the mass action law.[2]

As already detailed, the feed concentration of 3 meq·L^{-1} was chosen to fit the dynamic model of mass transfer resistances. It is noteworthy that when the feed concentration was composed by 93 % of zinc ions and 7 % of sodium ions a zinc uptake of 2.93 meq·g^{-1} was observed, while in a single feed concentration of 3 meq·L^{-1} of zinc ions, 2.5 meq·g^{-1} was the zinc uptake.[6] Then, it seems that sodium ions have promoted the zinc removal. An uptake of 2.5 meq·g^{-1} represents 64 % of the zeolite CEC. When the large cavities are occupied, this value reaches 69 % in Y zeolites.[2] Therefore, sodium ions may promote the diffusion of
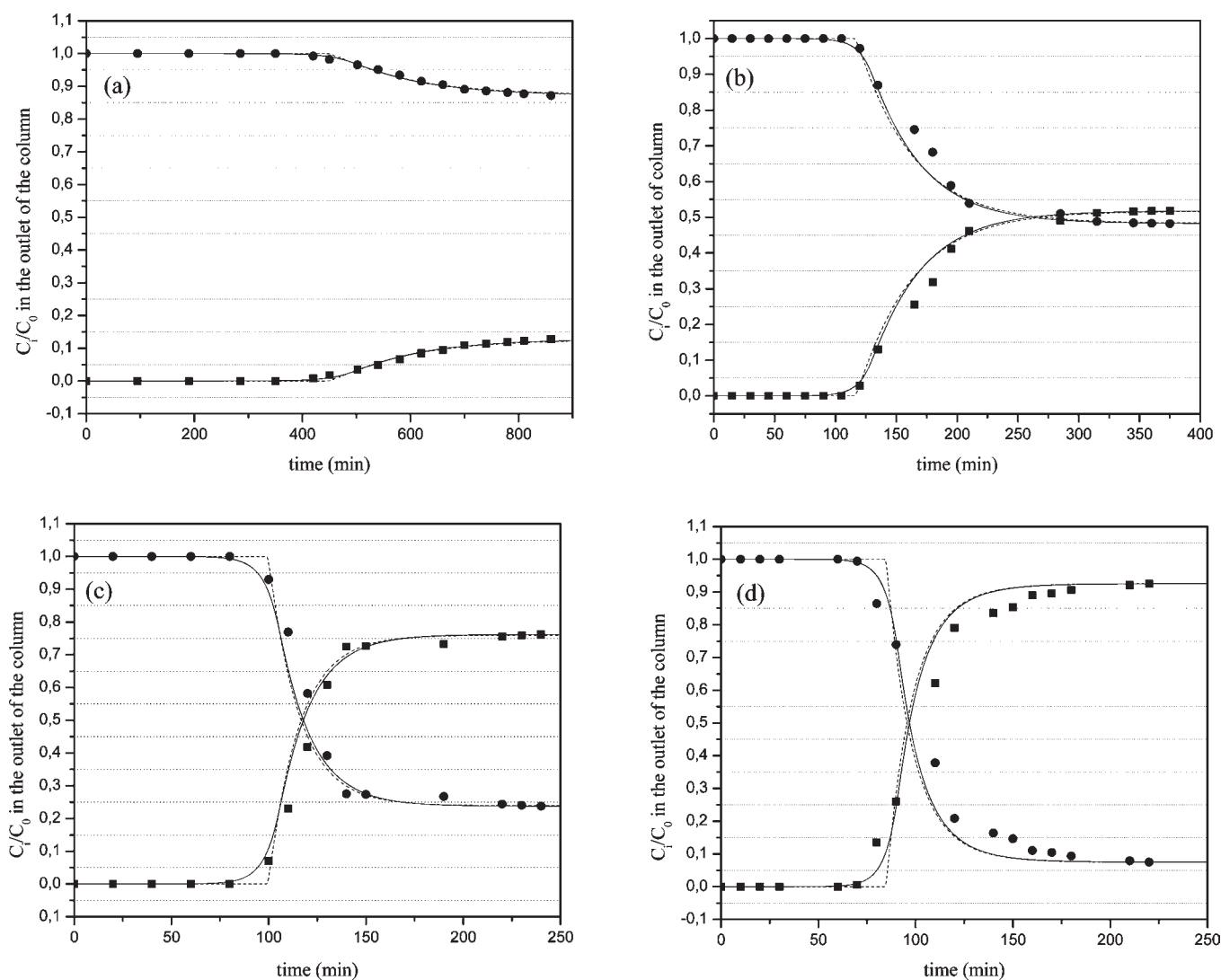
379

dx.doi.org/10.1021/je100568n |*J. Chem. Eng. Data* 2011, 56, 375–382

Figure 4. Experimental and calculated breakthrough curve for the ion exchange $Zn^{2+}-Na^{+}$. ●, experimental Zn^{2+}; ■, experimental Na^{+}; —, double resistance model; - - -, single resistance model: (a) $C_t = 3$ meq·L^{-1}, $X_{Zn} = 0.13$, $X_{Na} = 0.87$; (b) $C_t = 3$ meq·L^{-1}, $X_{Zn} = 0.52$, $X_{Na} = 0.48$; (c) $C_t = 3$ meq·L^{-1}, $X_{Zn} = 0.76$, $X_{Na} = 0.24$; (d) $C_t = 3$ meq·L^{-1}, $X_{Zn} = 0.93$, $X_{Na} = 0.07$.

zinc ions to less accessible sites. Still unpublished results show that this favorable behavior also happens with chromium ions. Probably sodium ions can facilitate the dehydration process of the higher charged ions. Then, such water molecules may diffuse easier to the bulk solution.

Dynamics of the Fixed-Bed Column. In Table 4, the quantity values of Zn^{2+} ions retained in the zeolite NaY through a mass balance (eq 1) and calculated by the mass action law are shown. In accordance to the observed deviations in Table 5, the mass action law is an efficient model to describe the equilibrium at the solid/liquid interface.

Several studies[18,19,22,24,25] have shown that the mass action law is efficient to represent equilibrium in ion exchange for different systems. However, the mass action law was used in some studies to represent the equilibrium in the dynamics of the fixed-bed column only.[9,31,32] Nevertheless, these works considered an ideal behavior that means that all sites are available to the exchanging process. At the end of the process, a monolayer of the in-going ions is formed. In other words, the theoretical cation exchange capacity is used totally. When zeolites are considered such a

model is not applicable due to its microporosity and steric problems faced by the in-going ion. Particularly Y zeolites have hexagonal prisms that are almost inaccessible to a great range of cations. Only small ions such as Ag^{+} (crystal radius of 1.26 Å and hydrated radius of 3.41 Å[33]) are able to diffuse and to be exchanged in sites located in such cavities.[34]

In both dynamic models used in this study, that is, intraparticle diffusion as the rate-controlling step and film and intraparticle diffusions as the rate-controlling steps, the mass transfer coefficient in the solid phase (K_{Si}) was obtained as described in the section Dynamic Modeling of Ion Exhange in a Fixed-Bed Column. Table 5 shows the values of these parameters.

Considering the values presented in Table 5, an almost linear relationship may be observed between the intraparticle mass transfer coefficient and zinc concentration in the feed solution. Such behavior was already seen[3,35] and probably is related to the driving force of the exchanging process, that is, the difference in the zinc amount in the fluid phase and in the equilibrium condition. The higher the concentration gradient, the faster the mass transfer process is.

In the mathematical model that considered the diffusion intraparticle addition, the diffusion through the external liquid film, the coefficient of mass transfer in the external liquid film was calculated by eqs 22 to 25. The value obtained was 280 min^{-1}. If such a value is compared to the intraparticle mass transfer coefficient, it may be concluded that the overall rate-controlling step is the intraparticle diffusion as $1/K_F < 1/K_S$. Quantitative values will be discussed later. In some way, such a conclusion was already expected since zeolite Y is a molecular sieve. Diffusion to supercages is relatively easy as hydrated ions can be well accommodated. On the other hand, sodalite cavities and mainly hexagonal prisms add a gradual difficulty in the diffusion and subsequent exchange process as the in-going ions need to dehydrate and some dehydration energy should be supplied by the system.[3]

The axial dispersion coefficient for both models was estimated as 0.48 cm$^2\cdot$min^{-1} through eq 21. The molecular diffusivity used in the calculations of the coefficient of mass transfer in the external film and the axial dispersion coefficient was 4.2×10^{-4} cm$^2\cdot$min^{-1}.[36]

In Figures 4a to 4d are presented the experimental and simulated breakthrough data. Both models represented the experimental data of breakthrough curves adequately; however, the model of dual resistance obtained the best description of the process in the early part of the curves. This shows that in the initial stage of ion exchange the diffusion in the external liquid film is the rate-controlling step. In the beginning of the ion exchange process there is a low amount of ions already exchanged. Therefore, even for a microporous system such as zeolite, the internal resistance seems to be negligible because most external ion exchange sites are still available. On the other hand, as ion exchange proceeds after the breakpoint and the bed starts to saturate, the cavities are more and more crowded. Then, intraparticle diffusion plays an important role and cannot be neglected.

It must be emphasized that the breakthrough data were obtained with the optimal flow rate of 8 mL·min^{-1}.[6] This means that all diffusional resistances are minimized. Again, as the exchanger is predominantly microporous, intraparticle resistance always exists. Then, it may be supposed that film resistance is minimized in the optimal operating conditions. If so, when the fixed-bed system is operated far from such conditions, a higher influence of film resistance in the whole breakthrough curve is expected.

It is outstanding that the same influence of resistance to mass transfer of the external liquid film in adsorption processes has been reported.[37−39] Then, it may happen in the ion exchange process as well.

Although in zinc uptake in NaY zeolite columns the initial stage seems to be controlled by film diffusion, the overall process of mass transfer is controlled by intraparticle diffusion.[37−39] In this work, this has been seen through the fact that the resistance is inversely proportional to the coefficient of mass transfer. Thus, to $1/K_{Fi}$ (1/280) and $1/K_{Si}$ (see Table 5) for any fraction of Zn^{2+} ions in feed concentration, we see that $1/K_{Fi} < 1/K_{Si}$. Thus, in the mathematical modeling of the dynamics of ion exchange between the Zn^{2+} and Na$^+$ ions in the fixed-bed column using zeolite NaY, both the ion diffusion in the external film and the ion diffusion in the solid phase should be considered.

■ CONCLUSIONS

This study investigated the ion exchange process between the cations Zn^{2+} and Na$^+$ in a fixed-bed column packed with zeolite NaY. The ion exchange mechanism was investigated through adjustment of experimental data to equilibrium and dynamic models. The models considered the effects of ion exchange equilibrium by the mass action law and the effects of mass transfer due to axial dispersion and external film resistance and intraparticle diffusion. The main conclusions to this study are:

- The equilibrium model (mass action law) adequately represented the experimental data of the equilibrium ion exchange.
- The initial stage of mass transfer in the dynamic ion exchange process is controlled by film resistance;.
- The overall process of mass transfer is intraparticle resistance, probably due to the operational conditions that allowed minimum film resistance.
- The zeolite NaY showed efficiency for the removal of the Zn^{2+} ion and can be used in the removal of Zn^{2+} in industrial effluents containing such metal.

■ AUTHOR INFORMATION

Corresponding Author
*Tel.: +55-44- 3011 4758. Fax: +55-44- 3011 4792. E-mail: indianaraostroski@hotmail.com.

■ REFERENCES

(1) Onganer, Y.; Temur, C. Adsorption dynamics of Fe(III) from aqueous solutions onto activated carbon. *J. Colloid Interface Sci.* **1993**, *205*, 241–244.

(2) Breck, D. W. *Zeolite molecular sieves*; Robert, E., Ed.; Krieger Publishing Company: Malabar, FL, USA, 1974.

(3) (^{a}) Barros, M. A. S. D.; Silva, E. A.; Arroyo, P. A.; Tavares, C. R. G.; Schneider, R. M.; Suszek, M.; Sousa-Aguiar, E. F. Removal of Cr(III) in the fixed bed column and batch reactors using as adsorbent zeolite NaX. *Chem. Eng. Sci.* **2004**, *59*, 5959–5966.

(4) (^{b}) Barros, M. A. S. D.; Arroyo, P. A.; Sousa-Aguiar, E.; Tavares, C. R. G. Thermodynamics of the exchange processes between K$^+$, Ca^{2+} and Cr^{3+} in zeolite A. *Adsorption* **2004**, *10*, 227–235.

(5) Kim, J. S.; Keane, M. A. The removal of iron and cobalt from aqueous solutions by ion exchange with nay zeolite: batch, semi − batch and continuous operation. *J. Chem. Technol. Biotechnol.* **2002**, *77*, 633–640.

(6) Ostroski, I. C.; Barros, M. A. S. D.; Silva, E. A.; Dantas, J. H.; Arroyo, P. A.; Lima, O. C. M. A comparative study for the ion exchange of Fe(III) and Zn(II) on zeolite NaY. *J. Hazard. Mater.* **2009**, *161*, 1404–1412.

(7) Pabalan, R.; Bertetti, F. Experimental and modeling study of ion-exchange between aqueous solutions and the zeolite mineral clinoptilolite. *J. Solution Chem.* **1999**, *28* (4), 367–393.

(8) Helfferich, F. *Ion exchange*; McGraw-Hill: New York, 1962.

(9) Ernest, M. V., Jr.; Whitley, R. D.; Ma, Z.; Linda Wang, N. H. Effects of mass action equilibria in fixed bed multicomponent ion exchange dynamics. *Ind. Eng. Chem. Res.* **1997**, *36*, 212–226.

(10) Bromley, L. A. Thermodynamic Properties on Strong Electrolytes in Aqueous Solutions. *AIChE J.* **1973**, *19* (2), 313–320.

(11) Wilson, G. M. Vapor−liquid equilibria XI. A new expression for the excess free energy of mixing. *J. Am. Chem. Soc.* **1964**, *86*, 127–130.

(12) Gazola, F. C.; Pereira, M. R.; Barros, M. A. S. D.; Silva, E. A.; Arroyo, P. A. Removal of Cr in fixed bed using zeolite NaY. *Chem. Eng. J.* **2006**, *117*, 253–261.

(13) Keane, M. A. The removal of copper and nickel from aqueous solution using Y zeolite ion exchangers. *Colloids Surf.* **1998**, *A 138*, 11–20.

(14) Borba, C. E.; Guirardello, R.; Silva, E. A.; Veit, M. T.; Tavares, C. R. G. Removal of nickel (II) ions from aqueous solution by biosorption in a fixed bed column: Experimental and theoretical breakthrough curves. *Biochem. Eng. J.* **2006**, *30*, 184–191.

(15) Raje, P.; Pinto, N. G. Combination of the steric mass action and non-ideal surface solution models for overload protein ion-exchange chromatography. *J. Chromatogr. A* **1997**, *760*, 89–103.

(16) Zemaitis, J. F., Jr.; Clar, D. M.; Rafal, M.; Scrivner, N. C. *Handbook of aqueous electrolyte thermodynamics*; American Institute of Chemical Engineers: New York, 1986.

(17) El Prince, A. M.; Babcock, K. L. Prediction of ion exchange equilibria in aqueous systems with more than two counterions. *Soil Sci.* **1975**, *120*, 332–338.

(18) Mehablia, M. A.; Shallcross, D. C.; Stevens, G. W. Ternary and quaternary ion exchange equilibria. *Solvent Extr. Ion Exch.* **1996**, *14* (2), 309–322.

(19) Petrus, R.; Warchol, J. Heavy metal removal by clinoptilolite. An equilibrium study in multi-component system. *Water Res.* **2005**, *39*, 819–830.

(20) Shallcross, D. C.; Herrmann, C. C.; Mccoy, B. J. An improved model for the prediction of multicomponent ion exchange equilibria. *Chem. Eng. Sci.* **1988**, *43* (2), 279–288.

(21) Smith, R. P.; Woodburn, E. T. Prediction of multicomponent ion exchange equilibria for the ternary system SO^{4-} - NO^{3-} - Cl^- from data of Binary Systems. *AIChE J.* **1978**, *24* (4), 577–586.

(22) Valverde, J. L.; De Lucas, A.; González, M.; Rodríguez, J. F. Equilibrium data for the exchange of Cu^{2+}, Cd^{2+}, and Zn^{2+} ions for H^+ on the cationic exchanger Amberlite IR-120. *J. Chem. Eng. Data* **2002**, *47*, 613–617.

(23) Vazquez Una, G. V.; Pampin, R. M.; Caeiro, R. B. Prediction del equilíbrio em sistemas ternários de intercambio iônico. *Anal. Quím. A* **1985**, *81*, 141–145.

(24) Shalcross, B. S.; Vo, D. C. Ion exchange equilibria data for systems involving H^+, Na^+, K^+, Mg^+, and Ca^{+2} ions. *J. Chem. Eng. Data* **2005**, *50*, 1018–1029.

(25) Shalcross, B. S.; Vo, D. C. Modeling solution phase behavior in multicomponent ion exchange equilibria involving H^+, Na^+, K^+, Mg^+, and Ca^{+2} ions. *J. Chem. Eng. Data* **2005**, *50*, 1995–2002.

(26) Nelder, J. A.; Mead, R. A simplex method for function minimization. *Comput. J.* **1965**, *7*, 308–315.

(27) Danckwerts, P. V. Continuous flow systems: distribution of residence times. *Chem. Eng. Sci.* **1953**, *2*, 1–13.

(28) Petzold, L. R. *A description of DASSL: A differential/algebric equation system solver*; STR, SAND: Livermore, 1982.

(29) Ruthven, D. M. *Principles of adsorption and adsorption process*; John Wiley & Sons: New York, 1984.

(30) Wilson, E. J.; Geankoplis, C. J. Liquid mass transfer at very low Reynolds numbers in packed beds. *Ind. Eng. Chem. Fundam.* **1966**, *5*, 1–9.

(31) Valverde, J. L.; De Lucas, A.; Carmona, M.; González, M.; Rodrýguez, J. F. A generalized model for the measurement of effective diffusion coeffcients of heterovalent ions in ion exchangers by the zero-length column method. *Chem. Eng. Sci.* **2004**, *59*, 71–79.

(32) Valverde, J. L.; De Lucas, A.; Carmona, M.; Pérez, J. P.; González, M.; Rodrýguez, J. F. Minimizing the environmental impact of the regeneration process of an ion exchange bed charged with transition metals. *Sep. Purif. Technol.* **2006**, *49*, 167–173.

(33) Nightingale, E. R., Jr. Phenomenological theory of ion solvation effective radii of hydrated ions. *J. Phys. Chem.* **1959**, *63*, 1381–1387.

(34) Fletcher, P.; Townsed, R. P. Exchange of hydrated amminate silver(I) ions in synthetic zeolites X, Y and modernite. *J. Chromatogr. A* **1980**, *201* (28), 93–105.

(35) Silva, E. A.; Cossich, E. S.; Tavares, C. R. G.; Filho, L. C.; Guirardello, R. Modeling of copper (II) biosorption by marine alga Sargassum sp. In fixed-bed column. *Process Biochem.* **2002**, *38*, 791–799.

(36) Lide, D. R.; Kehiaian, H. V. *CRC Handbook of Chemistry and Physics*, 7th ed.; CRC Press: Boca Raton, FL, 1996−1997.

(37) Ko, D. C. K.; Porter, J. F.; Mckay, G. Mass transport model for the fixed bed sorption of metals ions on bone char. *Ind. Eng. Chem. Res.* **2003**, *42*, 3458–3469.

(38) Liu, K. T.; Weber, W. J., Jr. Characterization of mass transfer parameters for adsorber modeling and design. *Process Res.* **1981**, *53*, 1541–1550.

(39) Zhang, L.; Lv., Y.; Wangc, K.; Rayb, A. K.; Zhao, X. S. Modeling of the adsorption breakthrough behaviors of Pb^{2+} in a fixed bed of ETS-10 adsorbent. *J. Colloid Interface Sci.* **2009**, *325*, 57–63.

382

dx.doi.org/10.1021/je100568n |*J. Chem. Eng. Data* 2011, 56, 375–382